Elliptical flow and isospin effects in heavy-ion collisions at intermediate energies

Sanjeev Kumar and Suneel Kumar*
School of Physics and Material Science, Thapar University, Patiala-147004, Punjab, India

Rajeev K. Puri
Department of Physics, Panjab University, Chandigarh-160014, India
(Received 25 October 2008; revised manuscript received 4 July 2009; published 27 January 2010)

The elliptical flow of fragments is studied for different systems at incident energies between 50 and 1000 MeV/nucleon using the isospin-dependent quantum molecular dynamics (IQMD) model. Our findings reveal that elliptical flow shows a transition from positive (in-plane) to negative (out-of-plane) values in the midrapidity region at a certain incident energy known as the transition energy. This transition energy is found to depend on the model ingredients, size of the fragments, and composite mass of the reacting system as well as on the impact parameter of the reaction. A reasonable agreement is observed for the excitation function of elliptical flow between the data and our calculations. Interestingly, the transition energy is found to exhibit a power-law mass dependence.

DOI: 10.1103/PhysRevC.81.014611 PACS number(s): 25.70.−z, 25.75.Ld, 21.65.Ef, 24.10.Lx

I. INTRODUCTION

Information about the nature of the equation of state is still a burning topic of present-day nuclear physics research in general and of research on heavy-ion collisions in particular. Quite good progress has been made in recent years in determining the nuclear equation of state from heavy-ion reactions [1,2]. Among different observables, collective flow enjoys a special status. This is due to its sensitive response to the model ingredients that define the equation of state. A lot of theoretical and experimental effort has been made in studying the collective flow in heavy-ion collisions [3–9]. This collective motion of the particles in a heavy-ion collision can be studied via directed and elliptical flows. The directed flow, which measures the collective motion of the particles in the reaction plane, has been studied extensively at the energies available at the LBNL Bevalac, GSI heavy-ion synchrotron (SIS), and BNL Alternating Gradient Synchrotron (AGS) [10]. This flow is reported to diminish at higher incident energies because of the large beam rapidity. Therefore, elliptical flow [11] is much more suited at these incident energies. The elliptical flow describes the eccentricity of an ellipse-like distribution. Quantitatively, it is the difference between the major and minor axis. The orientation of the major axis is confined to the azimuthal angle ϕ or $\phi + \frac{\pi}{2}$ for ellipse-like distribution. The major axis lies within the reaction plane for ϕ; while $\phi + \frac{\pi}{2}$ indicates that the orientation of the ellipse is perpendicular to the reaction plane, which is the case for squeeze-out flow and may be expected at midrapidity [12]. Therefore, the elliptical flow is defined by the second-order Fourier coefficient from the azimuthal distribution of detected particles at midrapidity. Mathematically,

$$\frac{dN}{d\phi} = p_0(1 + 2v_1 \cos\phi + 2v_2 \cos 2\phi). \quad (1)$$

Here, ϕ is the azimuthal angle between the transverse momentum of the particle and reaction plane. The positive value of the elliptical flow $\langle \cos 2\phi \rangle$ reflects an in-plane emission, whereas out-of plane emission is reflected by its negative value. The reason for the anisotropic flow is orthogonal asymmetry in the configuration space (noncentral collisions) and rescattering. In the case of elliptical flow, the initial "ellipticity" of the overlap zone is usually characterized by a quantity $\epsilon = \frac{\langle y^2 - x^2 \rangle}{\langle y^2 + x^2 \rangle}$, assuming the reaction plane is xz. As the system expands, spatial anisotropy decreases. From the above discussion, it is clear that the second-order flow (elliptical flow) is a better candidate for determining the nuclear equation of state than first-order sideward flow (directed flow).

In recent years, several experimental groups have measured elliptical flow. The FOPI, INDRA, and PLASTIC BALL Collaborations [4,5] are actively involved in measuring the excitation function of elliptical flow from Fermi energies to relativistic energies. In most of these studies, the $_{79}Au^{197} + _{79}Au^{197}$ reaction has been taken [4,5]. Interestingly, a change in the elliptical flow was reported from positive to negative values around 100 MeV/nucleon. Both the mean field and two-body binary collisions play an important role in this energy domain. The mean field is supposed to play a dominant role at low incident energies. The binary collisions start dominating the physics gradually. A detailed study of the excitation function of elliptical flow in the entire energy region can provide useful information about the nucleon-nucleon interactions related to the nuclear equation of state.

As discussed above, many attempts have already been made in the literature to explore different aspects of directed sideward flow. In this paper, we attempt to study the different aspects of elliptical flow v_2. For the present study, the isospin-dependent quantum molecular Dynamics (IQMD) model is used to generate the phase space of nucleons. The article is organized as follows. We discuss the model briefly in Sec. II. The results are discussed in Sec. III, and we summarize the results in Sec. IV.

*suneel.kumar@thapar.edu

II. ISOSPIN-DEPENDENT QUANTUM MOLECULAR DYNAMICS MODEL

The IQMD [13] model treats different charge states of nucleons, deltas, and pions explicitly [13], as inherited from the Vlasov-Uehling-Uhlenbeck (VUU) model [14]. The IQMD model has been used successfully for the analysis of a large number of observables from low to relativistic energies. The isospin degree of freedom enters into the calculations via symmetry potential, cross sections, and Coulomb interaction [14]. The details about the elastic and inelastic cross sections for proton-proton and neutron-neutron collisions can be found in Ref. [13].

In this model, baryons are represented by Gaussian-shaped density distributions

$$f_i(\vec{r},\vec{p},t) = \frac{1}{\pi^2\hbar^2}\exp\left(-[\vec{r}-\vec{r}_i(t)]^2\frac{1}{2L}\right) \times \exp\left(-[\vec{p}-\vec{p}_i(t)]^2\frac{2L}{\hbar^2}\right). \quad (2)$$

Nucleons are initialized in a sphere with radius $R = 1.12A^{1/3}$ fm, in accordance with the liquid-drop model. Each nucleon occupies a volume of h^3, so that phase space is uniformly filled. The initial momenta are randomly chosen between 0 and Fermi momentum (p_F). The nucleons of the target and projectile interact via two- and three-body Skyrme forces, the Yukawa potential, Coloumb interactions, and momentum dependent interactions. In addition to the use of explicit charge states of all baryons and mesons, a symmetry potential between protons and neutrons corresponding to the Bethe-Weizsacker mass formula has been included.

The hadrons propagate using Hamilton equations of motion:

$$\frac{d\vec{r}_i}{dt} = \frac{d\langle H\rangle}{d\vec{p}_i};\quad \frac{d\vec{p}_i}{dt} = -\frac{d\langle H\rangle}{d\vec{r}_i}, \quad (3)$$

with

$$\begin{aligned}\langle H\rangle &= \langle T\rangle + \langle V\rangle \\ &= \sum_i \frac{p_i^2}{2m_i} + \sum_i\sum_{j>i}\int f_i(\vec{r},\vec{p},t)V^{ij}(\vec{r}\,',\vec{r}) \\ &\quad \times f_j(\vec{r}\,',\vec{p}\,',t)d\vec{r}d\vec{r}\,'d\vec{p}d\vec{p}\,'. \end{aligned} \quad (4)$$

The baryon-baryon potential V^{ij}, in the above relation, reads as

$$\begin{aligned} V^{ij}(\vec{r}\,'-\vec{r}) &= V^{ij}_{\rm Skyrme} + V^{ij}_{\rm Yukawa} + V^{ij}_{\rm Coul} + V^{ij}_{\rm mdi} + V^{ij}_{\rm sym} \\ &= \left[t_1\delta(\vec{r}\,'-\vec{r}) + t_2\delta(\vec{r}\,'-\vec{r})\rho^{\gamma-1}\left(\frac{\vec{r}\,'+\vec{r}}{2}\right)\right] \\ &\quad + t_3\frac{\exp(|\vec{r}\,'-\vec{r}|/\mu)}{(|\vec{r}\,'-\vec{r}|/\mu)} + \frac{Z_iZ_je^2}{|\vec{r}\,'-\vec{r}|} \\ &\quad + t_4\ln^2[t_5(\vec{p}_i\,'-\vec{p})^2+1]\delta(\vec{r}\,'-\vec{r}) \\ &\quad + t_6\frac{1}{\varrho_0}T_3^iT_3^j\delta(\vec{r}_i\,'-\vec{r}_j). \end{aligned} \quad (5)$$

Here Z_i and Z_j denote the charges of the ith and jth baryon, and T_3^i and T_3^j are their respective T_3 components (i.e., 1/2 for protons and −1/2 for neutrons). The meson potential consists of the Coulomb interaction only. The parameters μ and $t_1,\ldots,t_6$ are adjusted to the real part of the nucleonic optical potential. For the density dependence of the nucleon optical potential, standard Skyrme-type parametrization is employed. The momentum dependence $V^{ij}_{\rm mdi}$ of the N-N interactions, which may optionally be used in IQMD, is fitted to experimental data in the real part of the nucleon optical potential. The choice of equation of state (or compressibility) is still a controversial one. Many studies advocate softer matter, whereas many more believe the matter to be harder in nature [14,15]. As noted [16], elliptical flow is unaffected by the choice of equation of state. For the present analysis, a hard (H) and hard momentum dependent (HMD) equation of state, has been employed along with the standard energy-dependent cross section.

III. RESULTS AND DISCUSSION

We here perform a complete systematic study for the mass range between 80 and 394 units and over the full range of the impact parameter. We here simulate the reactions of ${}_{20}Ca^{40} + {}_{20}Ca^{40}$, ${}_{28}Ni^{58} + {}_{28}Ni^{58}$, ${}_{41}Nb^{93} + {}_{41}Nb^{93}$, ${}_{54}Xe^{131} + {}_{54}Xe^{131}$, and ${}_{79}Au^{197} + {}_{79}Au^{197}$ at incident energies between 50 and 1000 MeV/nucleon. In addition, the reactions of ${}_{40}Zr^{96} + {}_{40}Zr^{96}$ and ${}_{44}Ru^{96} + {}_{44}Ru^{96}$ are also simulated to check the isospin effects explicitly. As noted in Ref. [17], the relativistic effects do not play a role at these incident energies, and the intensity of subthreshold particle production is very small. The phase space generated by the IQMD model has been analyzed using the minimum spanning tree (MST) [2,18] method. The MST method binds two nucleons in a fragment if their distance is less than 4 fm. In recent years, several improvements have also been suggested [19]. One of the improvements is to also imply a momentum cut of the order of Fermi momentum. This method is dubbed as the MSTM method. The entire calculations are performed at $t = 200$ fm/c. This time is chosen by keeping in view the saturation of the collective flow [8].

The elliptical flow is defined as the average difference between the square of the x and y components of the particle's transverse momentum. Mathematically, it can be written as

$$v_2 = \left\langle \frac{p_x^2 - p_y^2}{p_x^2 + p_y^2} \right\rangle, \quad (6)$$

where p_x and p_y are the x and y components of the momentum. The p_x is in the reaction plane, while p_y is perpendicular to the reaction plane.

A positive value of the elliptical flow describes the eccentricity of an ellipse-like distribution and indicates in-plane enhancement of the particle emission, i.e., a rotational behavior. On the other hand, a negative value of v_2 shows the squeeze-out effects perpendicular to the reaction plane. Obviously, zero value corresponds to an isotropic distribution in the transverse plane. The v_2 is generally extracted from the midrapidity region. The particles corresponding to $Y_{\rm c.m.}/Y_{\rm beam} > 0.1$ have been defined as projectile-like (PL),

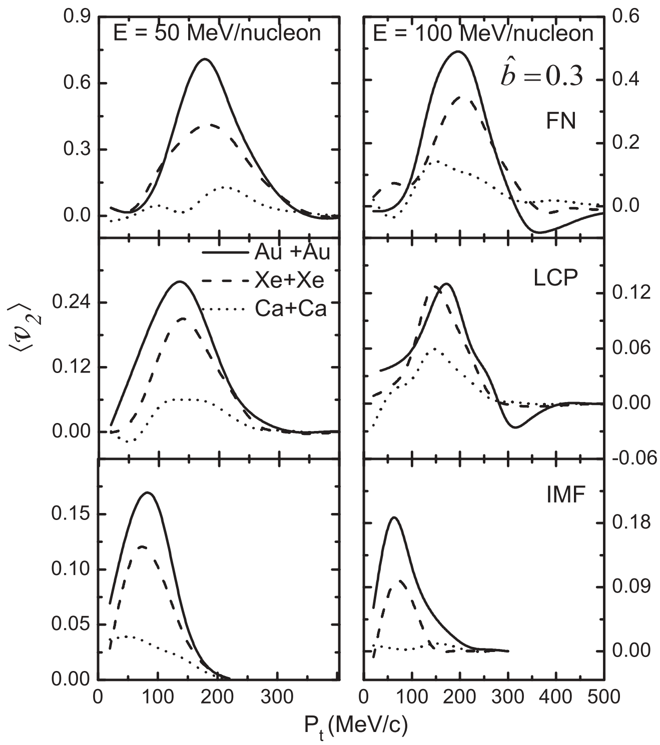

FIG. 1. Transverse momentum dependence of the elliptical flow, summed over the entire rapidity distribution, at $\hat{b} = 0.3$ for different symmetric reactions at 50 (left) and 100 (right) MeV/nucleon. The top, middle, and bottom panels represent the free nucleons (FN's), light charged particles (LCP's), and intermediate mass fragments (IMF's), respectively.

whereas $Y_{\rm c.m.}/Y_{\rm beam} < -0.1$ constitutes the target-like (TL) particles.

In Fig. 1, the final-state elliptical flow is displayed for the free particles (upper panel), light charged particles (LCP's) $[2 \leqslant A \leqslant 4]$ (middle), and intermediate mass fragments (IMF's) $[5 \leqslant A \leqslant A_{\rm tot}/6]$ (lower panel) as a function of transverse momentum (P_t). A Gaussian-type behavior is observed in all cases. Note that this elliptical flow is integrated over the entire rapidity range. This Gaussian-type behavior is quite similar to the one obtained by Colona *et al.* [20]. One sees that elliptical flow is positive in the whole range of P_t. Collective rotation is one of the main mechanisms for inducing the positive elliptical flow [21]. It is also evident from the figure that the peak of the Gaussian shifts toward lower values of P_t for heavier fragments. This is because the free and light charged particles feel the mean field directly, while heavy fragments have weaker sensitivity [22]. Furthermore, the peak values of v_2 for the free nucleons and LCP's at 50 MeV/nucleon is 0.70, 0.411, 0.126; and 0.27, 0.20, and 0.059 for the reactions of ${}_{79}\mathrm{Au}^{197} + {}_{79}\mathrm{Au}^{197}$, ${}_{54}\mathrm{Xe}^{131} + {}_{54}\mathrm{Xe}^{131}$, and ${}_{20}\mathrm{Ca}^{40} + {}_{20}\mathrm{Ca}^{40}$, respectively; the corresponding ratios are $\approx$5.0, 3.3, and 1. The mass ratios of these reactions are 4.93, 3.27, and 1, whereas the N/Z ratios are 1.49, 1.42, and 1. The v_2 ratios are in closer agreement with the system mass ratios. The results, however, are different at $E =$ 100 MeV/nucleon. Note that the peak values for the free nucleon are 0.48, 0.34, and 0.134; and for LCP's, the numbers are 0.132, 0.125, and 0.058. Their corresponding ratios are $\approx$2.92, 2.36, and 1, indicating a clear deviation from the mass ratio.

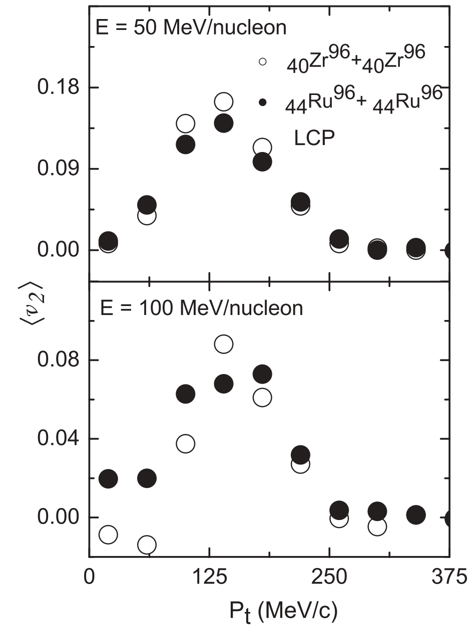

FIG. 2. Transverse momentum dependence of the elliptical flow, summed over entire rapidity distribution, for LCP's at 50 (top) and 100 MeV/nucleon (bottom), respectively. The reactions under study having same mass number and different atomic number. The reactions are analyzed with MSTM algorithm.

To further strengthen our interpretation of the estimated v_2 ratios, we display in Fig. 2 the reactions of ${}_{40}\mathrm{Zr}^{96} + {}_{40}\mathrm{Zr}^{96}$ and ${}_{44}\mathrm{Ru}^{96} + {}_{44}\mathrm{Ru}^{96}$ under the same conditions for LCP's. These reactions are analyzed within the MST method with the momentum cut. Interestingly, the N/Z effect is more visible at $E = 100$ MeV/nucleon, indicating that this difference is not due to the mass dependence alone, but is also due to the isospin effect. Our findings are also supported by Zhang *et al.* [23], who showed that a neutron-rich system exhibits weaker squeeze-out flow. At low incident energy (say, 50 MeV/nucleon), binary collisions are rare, therefore isospin in the mean field does not play a role. On the other hand, around 100 MeV/nucleon, the isospin effects of the both mean field and binary collisions contribute, making isospin maximum. At higher incident energies, the role of the mean field reduces. This situation is similar to the intermediate mass fragments, where the maximum value is obtained around 100 MeV/nucleon [24].

To further understand the origin of this isospin effect, the transverse momentum dependence of elliptical flow for target-like, midrapidity, and projectile-like distributions is displayed in Fig. 3. From the figure, we see that the isospin effect originates from the midrapidity region or in other words from the participant zone. It is also clear that the isospin effects are stronger for LCP's than for other fragments. This is because heavier fragments have weak sensitivity toward the mean field [22].

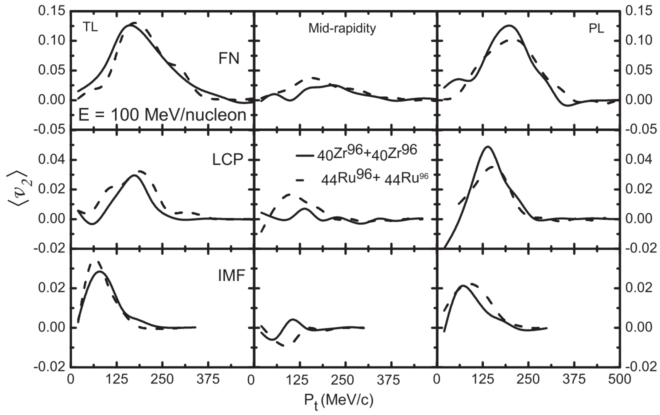

FIG. 3. Transverse momentum dependence of the elliptical flow at $E = 100$ MeV/nucleon for the reactions displayed in Fig. 2. The left, middle, and right panels represent the target-like, midrapidity, and projectile-like distributions, respectively; the top, middle, and bottom panels have the same meaning as in Fig. 1. The reactions are analyzed with the MST algorithm.

In Fig. 4, we display the transverse momentum dependence of elliptical flow for LCP's in the midrapidity region with and without symmetry energy. The effect of symmetry energy is clearly visible in the figure. This is in agreement with the findings of Chen *et al.* [25], where it was concluded that light cluster production acts as a probe for symmetry energy. This strengthens our agreement that elliptical flow depends on the N/Z ratio or, alternatively, the isospin dependence rather than on the size of the interacting system.

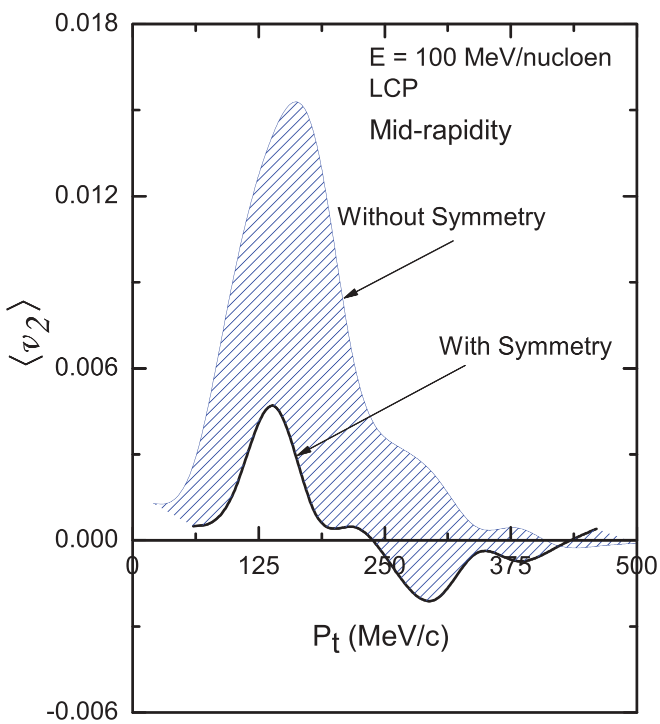

FIG. 4. (Color online) Transverse momentum dependence of elliptical flow for LCP's in the midrapidity region at $E = 100$ MeV/nucleon. The panel exhibits the effect of symmetry energy on the $_{40}Zr^{96} + _{40}Zr^{96}$ reaction.

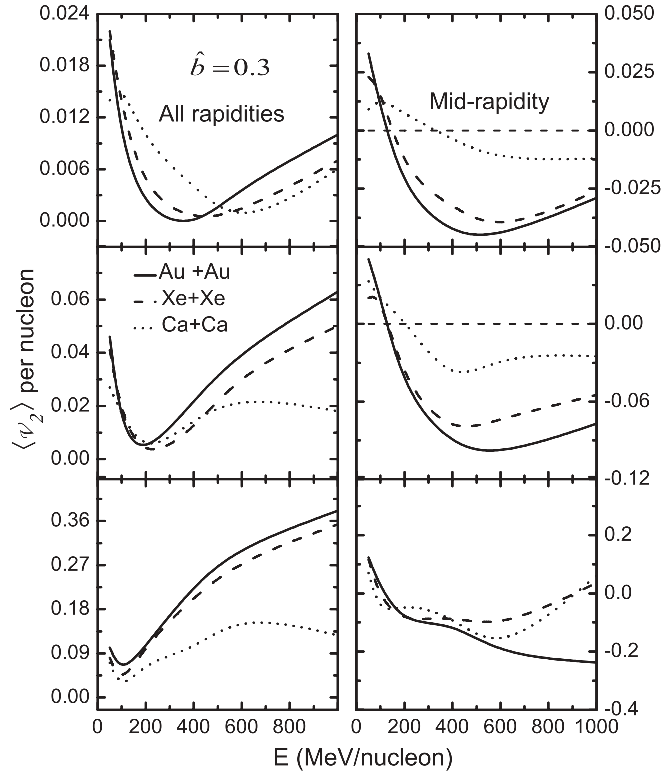

FIG. 5. Variation of the elliptical flow, summed over the entire transverse momentum, with beam energy at $\hat{b} = 0.3$ for different symmetric reactions over the entire rapidity range (left panels) and at midrapidity (right panels). The top, middle, and bottom panels have the same meanings as in Fig. 1.

In Fig. 5, we display the variation of the excitation function of elliptical flow v_2 for free nucleons, LCP's, and IMF's over the entire rapidity and midrapidity region. The elliptical flow is found to become less positive (entire rapidity) or more negative (midrapidity) with the increase in the beam energy, up to a certain energy, and then again becomes more positive or less negative. This is because the spectators move faster after v_2 reaches a minimum value [5]. The energy at which the behavior changes is found to decrease with the size of the fragment. This means that the flow of heavier fragments is larger than that of LCP's and free nucleons at all beam energies. These type of findings are also reported by different authors in Ref. [16]. This is true for the entire rapidity region as well as for the midrapidity region.

The interesting phenomenon of transition from in-plane to out-of-plane is observed at the midrapidity region [4,26], while no transition is observed when integrated over the entire rapidity region. The energy at which this transition is observed is dubbed as the transition energy E_{Trans}. It means that participant zone is responsible for the transition from in-plane to out-of-plane. That is why free particles and LCP's, which originate from the participant zone, show a systematic behavior with the beam energy as well as with the composite mass of the system. The elliptical flow for these particles is found to become more negative with the increase in the composite mass of the system. The heavier the system, the greater the Coulomb repulsion and the more negative is the elliptical flow. This

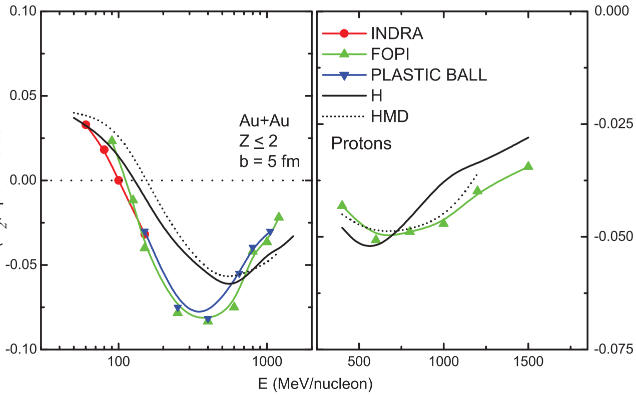

FIG. 6. (Color online) Variation of the elliptical flow, summed over the entire transverse momentum, with beam energy at $|y| = |\frac{y_{c.m.}}{y_{beam}}| \leqslant 0.1$ for the ${}_{79}Au^{197} + {}_{79}Au^{197}$ reaction. Here a comparison is shown with the experimental findings of the INDRA, FOPI, and PLASTIC BALL Collaborations [4–6].

systematics of E_{Trans} with the composite mass of the system is discussed later.

In Fig. 6, we show v_2 at midrapidity ($|y| = |\frac{y_{c.m.}}{y_{beam}}| \leqslant 0.1$) for $Z \leqslant 2$ (left panel) and for protons (right panel) as a function of the incident energy. The rapidity cut is in accordance with the experimental findings. The theoretical results are compared with the experimental data extracted by INDRA, FOPI, and PLASTIC BALL Collaborations [4–6]. With the increase in the incident energy, elliptical flow v_2 changes from positive to negative values exhibiting a transition from the in-plane to out-of-plane emission of nucleons. This is because the mean field, which contributes to the formation of a rotating compound system, becomes less important, and the collective expansion process based on nucleon-nucleon scattering starts to be predominant. This competition between the mean field and N-N collisions depends strongly on the effective interactions, which lead to the different transition energies due to different equations of state. Because of the repulsive nature of the momentum dependent interactions, which leads to the suppression of binary collisions, less squeeze-out is observed in the presence of momentum dependent interactions (HMD) compared to the static one (H). The maximal negative value of v_2 is obtained around $E = 500$ MeV/nucleon with hard (H) and hard momentum dependent (HMD) equations of state. This out-of-plane emission decreases again toward the higher incident energies. This happens because of the faster movement of the spectator matter after v_2 reaches the maximal negative value [5]. This trend is in agreement with experimental findings. A close agreement with data is obtained in the presence of a hard equation of state for $Z \leqslant 2$ particles, and in the presence of momentum dependent interactions for protons. Similar results and trends have also been reported by Zhang *et al.* in their recent communication [26].

The investigation of the elliptical flow with scaled impact parameter over the entire rapidity range is displayed in Fig. 7. Here the top, middle, and bottom panels represent the free nucleons, LCP's, and IMF's. The value of the elliptical flow v_2 becomes more positive with the impact parameter and composite mass of the system at $E = 50$ MeV/nucleon, while

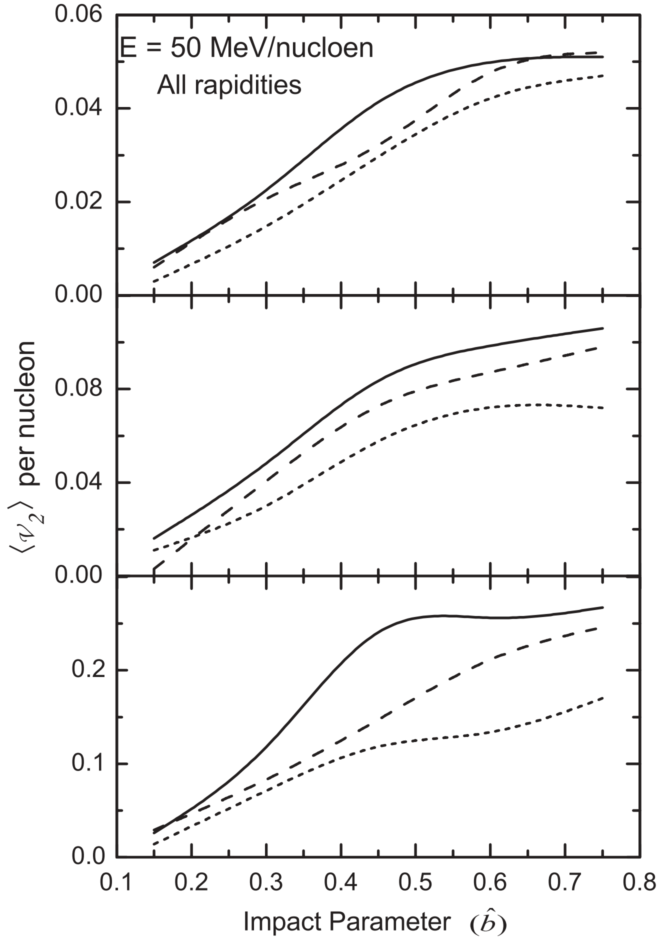

FIG. 7. Impact parameter dependence of the elliptical flow, summed over the entire transverse momentum and rapidity distribution, at incident energies 50 MeV/nucleon. The top, middle, and bottom panels are for free particles, LCP's and IMF's, respectively.

at higher energies (not shown here), it is found to become less positive (entire rapidity) or more negative (midrapidity) with the composite mass of the system. This indicates the dominance of the in-plane flow at low incident energies with increasing impact parameter and composite mass of the system. Moreover, dominance of the out-of-plane flow at higher energies with small impact parameter and composite mass of the system is observed. With the increase in the beam energy, the expansion of the compressed zone becomes more vigorous; while with an increase in the impact parameter, the participant zone decreases, resulting in an increase in the spectator region, indicating the dominance of azimuthal anisotropy with impact parameter. On the other hand, it reduces with beam energy. These observations are consistent with the experimental findings and with other theoretical works [16,21,27].

Finally, we carry out the system size dependence of the elliptical flow for free nucleons and LCP's. In Fig. 8, we show the transition energy E_{Trans} as a function of the composite mass of the system for free nucleons and LCP's. From the figure, we see that the transition energy decreases with the composite mass of the system as well as with the size of the fragment. The reason for this is that the pressure produced by the Coloumb

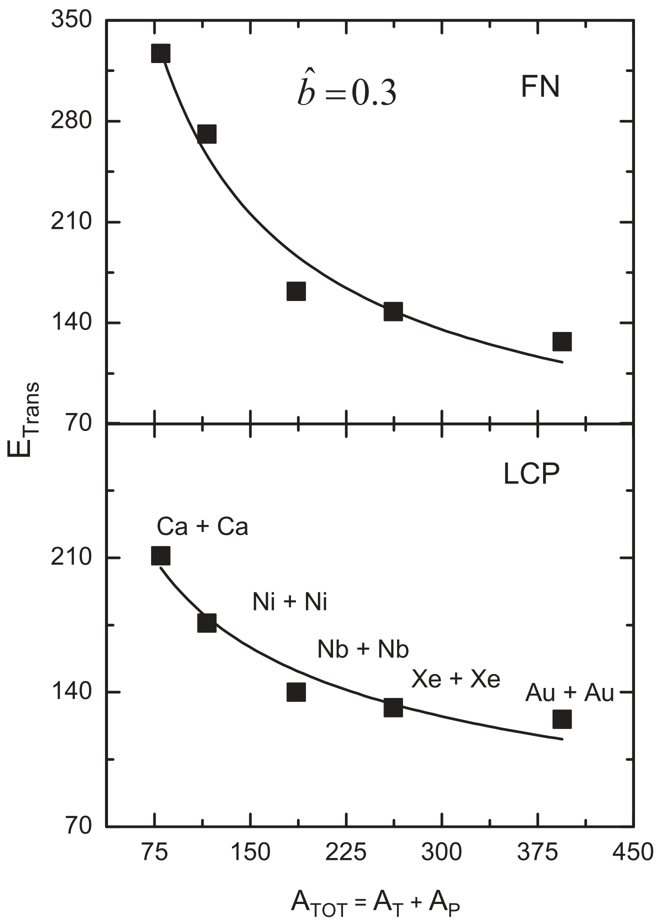

FIG. 8. Transition energies (E_{Trans} in MeV/nucleon) for elliptical flow as a function of the combined mass of the system. The upper panel is for the free nucleons, while lower panel is for the LCP's.

interactions increases with the system size. This dependence can be fitted using a power law of the kind

$$E_{\text{Trans}} = C\left(A_{\text{tot}}^{-\tau}\right). \tag{7}$$

The exponent τ is found to be two times larger for free particles (0.67) than for LCP's (0.35). This exponent is quite smaller than the exponent of the balance energy in directed flow [26]. This is due to the different origin of the balance and transition energies. The balance energy counter balances the mean field and N-N collisions, while transition energy is due to the more complex effects such as expansion of the compressed zone and shadowing of the cold spectator matter.

IV. CONCLUSION

In conclusion, we have investigated the elliptical flow of fragments for different reacting systems at incident energies between 50 and 1000 MeV/nucleon using the isospin-dependent quantum molecular dynamics (IQMD) model. The elliptical flow is found to show a transition from in-plane to out-of-plane at a certain beam energy in the midrapidity region, while no such transition is observed when integrated over the entire rapidity region. This transition energy is found to decrease with the composite mass as well as with the size of the fragment. The transition energy is further parametrized in term of mass power law. In addition, LCP's exhibit an isospin effect in the midrapidity region.

ACKNOWLEDGMENTS

This work has been supported by the Grant No. 03(1062)06/EMR-II, from the Council of Scientific and Industrial Research (CSIR) New Delhi, Government of India.

[1] P. Danielewicz, R. Lacey, and W. G. Lynch, Science **298**, 1592 (2002); H. Stöcker and W. Greiner, Phys. Rep. **137**, 277 (1986); W. Reisdorf and H. G. Ritter, Annu. Rev. Nucl. Sci. **47**, 663 (1997); C. Hartnack and J. Aichelin, Phys. Rev. C **49**, 2801 (1994); S. Kumar, S. Kumar, and R. K. Puri, *ibid.* **78**, 064602 (2008); A. R. Raduta and F. Gulminelli, *ibid.* **75**, 024605 (2007).

[2] J. Aichelin, Phys. Rep. **202**, 233 (1991).

[3] G. D. Westfall *et al.*, Phys. Rev. Lett. **71**, 1986 (1993); M. B. Tsang *et al.*, Phys. Rev. C **53**, 1959 (1996); Y. M. Zheng, C. M. Ko, B. A. Li, and B. Zhang, Phys. Rev. Lett. **83**, 2534 (1999); A. B. Larionov, W. Cassing, C. Greiner, and U. Mosel, Phys. Rev. C **62**, 064611 (2000); B. A. Li, A. T. Sustich, and B. Zhang, *ibid.* **64**, 054604 (2001); C. Alt *et al.*, *ibid.* **68**, 034903 (2003).

[4] J. Lukasik, G. Auger, M. L. Begemann-Blaich *et al.*, Phys. Lett. **B608**, 223 (2005).

[5] A. Andronic *et al.*, Nucl. Phys. **A679**, 765 (2001); Phys. Lett. **B612**, 173 (2005).

[6] J. Lukasik *et al.* (INDRA Collaborations), presented at the International Workshop on Multifragmentation and Related Topics (IWM 2003), Caen, France, 2003 (unpublished).

[7] S. Kumar, M. K. Sharma, R. K. Puri, K. P. Singh, and I. M. Govil, Phys. Rev. C **58**, 3494 (1998); A. D. Sood, R. K. Puri, and J. Aichelin, Phys. Lett. **B594**, 260 (2004).

[8] A. D. Sood and R. K. Puri, Phys. Rev. C **69**, 054612 (2004); Eur. Phys. J. A **30**, 571 (2006).

[9] L. W. Chen and C. M. Ko, Phys. Lett. **B634**, 205 (2006); Phys. Rev. C **73**, 014906 (2006).

[10] M. Gyulassy, K. A. Frankel, and H. Stöcker, Phys. Lett. **B110**, 185 (1982); P. Danielewicz and M. Gyulassy, *ibid.* **B129**, 283 (1983); C. M. Ko and G. Q. Li, J. Phys. G: Nucl. Part. Phys. **22**, 1673 (1996); G. Q. Li, C. M. Ko, and B. A. Li, Phys. Rev. Lett. **74**, 235 (1995); G. Q. Li and C. M. Ko, Nucl. Phys. **A594**, 460 (1995); B. A. Li and C. M. Ko, Phys. Rev. C **52**, 2037 (1995); **58**, R1382 (1998); Nucl. Phys. **A601**, 457 (1996).

[11] H. Sorge, Phys. Rev. Lett. **78**, 2309 (1997); J. Y. Ollitrault, Phys. Rev. D **46**, 229 (1992).

[12] S. Voloshin and Y. Zhang, Z. Phys. C **70**, 665 (1996).

[13] C. Hartnack *et al.*, Eur. Phys. J. A **1**, 151 (1998).

[14] H. Kruse, B. V. Jacak, and H. Stöcker, Phys. Rev. Lett. **54**, 289 (1985); J. J. Molitoris and H. Stöcker, Phys. Rev. C **32**, 346(R) (1985); J. Aichelin and G. Bertsch, *ibid.* **31**, 1730 (1985).

[15] D. J. Magestro, W. Bauer, and G. D. Westfall, Phys. Rev. C **62**, 041603(R) (2000); E. Lehmann *et al.*, Z. Phys. A **355**, 55 (1996); A. D. Sood and R. K. Puri, Phys. Rev. C **73**, 067602 (2006); **70**, 034611 (2004).
[16] H. Y. Zhang *et al.*, J. Phys. G: Nucl. Part. Phys. **28**, 2397 (2002).
[17] E. Lehmann, R. K. Puri, A. Faessler, G. Batko, and S. W. Huang, Prog. Part. Nucl. Phys. **30**, 219 (1993); Phys. Rev. C **51**, 2113 (1995).
[18] Y. K. Vermani and R. K. Puri, Europhys. Lett. **85**, 62001 (2009); Y. K. Vermani, S. Goyal, and R. K. Puri, Phys. Rev. C **79**, 064613 (2009); Y. K. Vermani and R. K. Puri, J. Phys. G: Nucl. Part. Phys. **36**, 105103 (2009); S. Kumar, R. K. Puri, and J. Aichelin, Phys. Rev. C **58**, 1618 (1998); R. K. Puri and J. Aichelin, J. Comput. Phys. **162**, 245 (2000); J. Singh, S. Kumar, and R. K. Puri, Phys. Rev. C **62**, 044617 (2000); R. K. Puri, C. Hartnack, and J. Aichelin, *ibid.* **54**, R28 (1996).
[19] J. Singh and R. K. Puri, Phys. Rev. C **62**, 054602 (2000).
[20] M. Colona, M. D. Toro, G. Ferini, and V. Greco, in Proceedings of the Catania Workshop on Nucleon and Neutrino Astrophysics, 15–16 Feb. 2007 (unpublished); M. Di Toro, S. J. Yennello, and B. A. Li, Eur. Phys. J. A **30**, 153 (2006).
[21] Y. G. Ma, W. Q. Shen, J. Feng, and Y. Q. Ma, Phys. Rev. C **48**, R1492 (1993); Z. Phys. A **344**, 469 (1993); Y. G. Ma, W. Q. Shen, and Z. Y. Zhu, Phys. Rev. C **51**, 1029 (1995); W. Q. Shen *et al.*, Nucl. Phys. **A551**, 333 (1993); R. Lacey *et al.*, Phys. Rev. Lett. **70**, 1224 (1993).
[22] T. Z. Yan *et al.*, Chin. Phys. **16**, 2676 (2007).
[23] F. S. Zhang, L. W. Chen, W. F. Li, and Z. Y. Zhu, Eur. Phys. J. A **9**, 149 (2000).
[24] M. B. Tsang *et al.*, Phys. Rev. Lett. **71**, 1502 (1993).
[25] L. W. Chen, C. M. Ko, and B. A. Li, Phys. Rev. C **68**, 017601 (2003).
[26] Y. Zhang and Z. Li, Phys. Rev. C **74**, 014602 (2006).
[27] J. Peter *et al.*, Nucl. Phys. **A519**, 611 (1990); Z. Y. He *et al.*, *ibid.* **A598**, 248 (1996).